Convergent Divergent Nozzle Flow Experiment

Samuel A. Masten, Tobias Hullette, Jarrad Harland
North Carolina State University MAE Department, Raleigh, NC, 27606

This experiment looks at pressure, temperature, and other thermodynamic variables when obtained from isentropic equations and from a converging-diverging (CD) nozzle flow setup. The objectives are to design and test a CD nozzle, calculate variations along the centerline of the CD nozzle at choked flow conditions, conduct an experiment to acquire pressure and temperature data, calculate Mach number variations along the centerline and exit of the CD nozzle, and analyze differences between the analytical and experimental results.

Nomenclature

A = nozzle area [mm^2]
A^* = nozzle area at choked flow condition [mm^2]
a = speed of sound [m/s]
M = Mach number
$\dot{m}$ = mass flow rate [kg/s]
p = pressure [Pa]
p_0 = stagnation pressure [Pa]
p_{01} = absolute pressure from tank [Pa]
p_{02} = absolute pressure from pitot tube [Pa]
ρ = density of fluid [kg/m^3]
ρ_0 = stagnation density [kg/m^3]
R = ideal gas constant [J/kg-K]
r = nozzle radius [mm]
T = temperature [K]
T_0 = stagnation temperature [K]
T_{01} = temperature from tank [K]
T_{02} = temperature from pitot tube [K]
T^* = temperature at choked flow condition [K]
V = flow velocity [m/s]
γ = ratio of specific heats

I. Introduction

This lab report presents the results for the final project in MAE 352 - Experimental Aerodynamics II Lab 4, which involved designing and manufacturing a CD nozzle using 3D printing technique. The objective was to conduct analytical calculations and numerical simulations on a designed CD nozzle required to reach supersonic speeds at the exit. These preliminary calculations were to be validated through experimentation using a 3D printed CD nozzle with the same geometry. Given constraints on the CD nozzle geometry included nozzle length, wall thickness, throat radius, and exit radius, which had to be within certain ranges. Additionally, the maximum air pressure supplied by the external tank was limited to 99 psi.

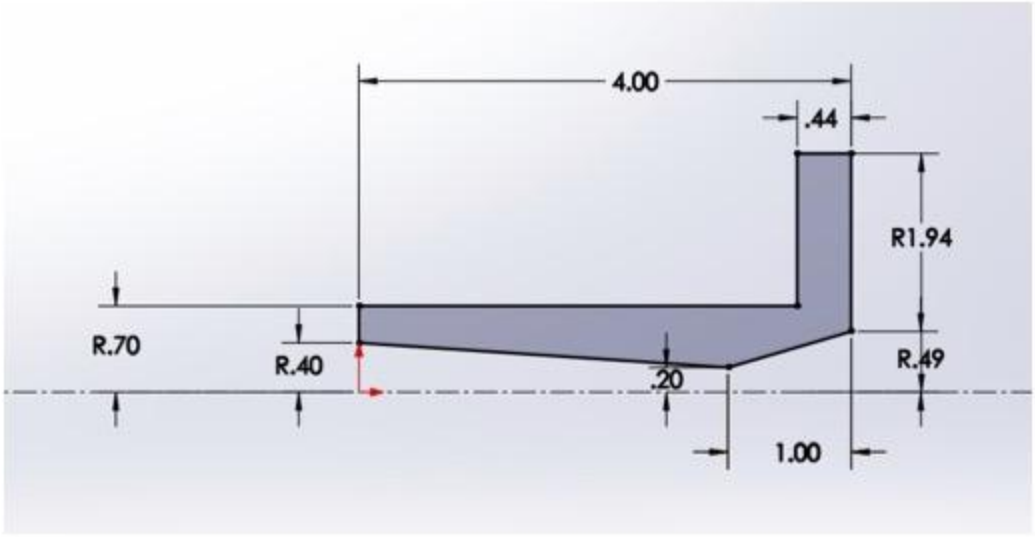

Figure 1. 2-D Axisymmetric Designed CD Nozzle with Dimensions

First, flow properties were determined via analytical means to fill up Table 1 using the geometry of the designed CD nozzle at the choked flow condition. Fluent, a CFD software provided by ANSYS was then used to computationally validate our design prior to manufacturing and analytical testing. Figures 2-5 illustrate anticipated trends in flow properties for the designed CD nozzle; specifically the static pressure and temperature will continue to decrease as the velocity increases.

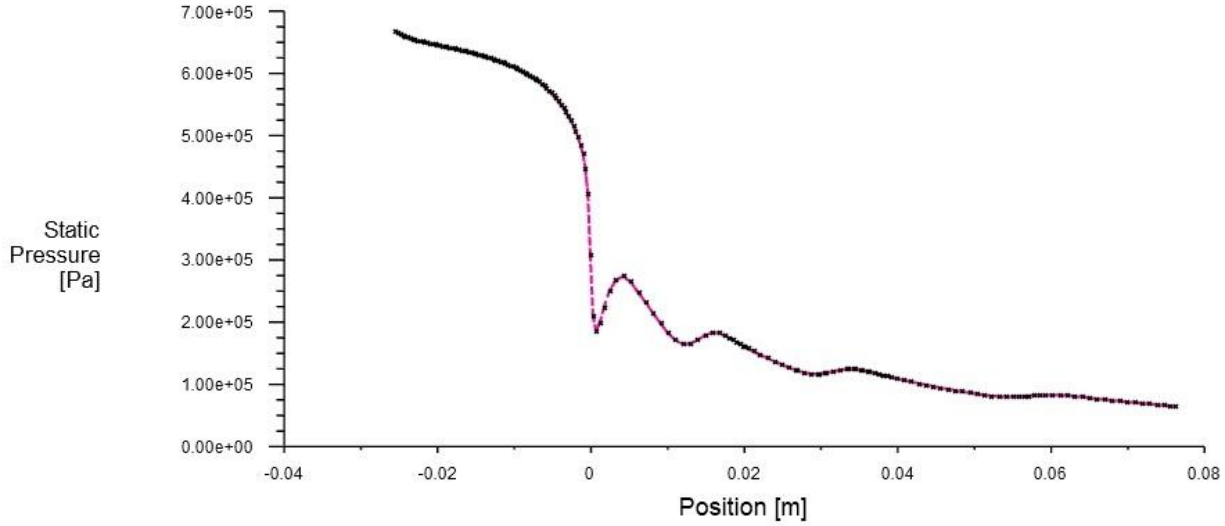

Figure 2. Static Pressure Curve Plotted as a Function of the Flow Position within the Nozzle (The throat exists at x = 0m).

The wavelike motion occurring following the throat location is due to changes in pressure caused by shocks occurring in the flow downstream. This same phenomenon can be seen in the below contours. The subtle blending

of colors is due to expansion waves in the flow indicating areas of slightly differing pressures, temperatures, or speed.

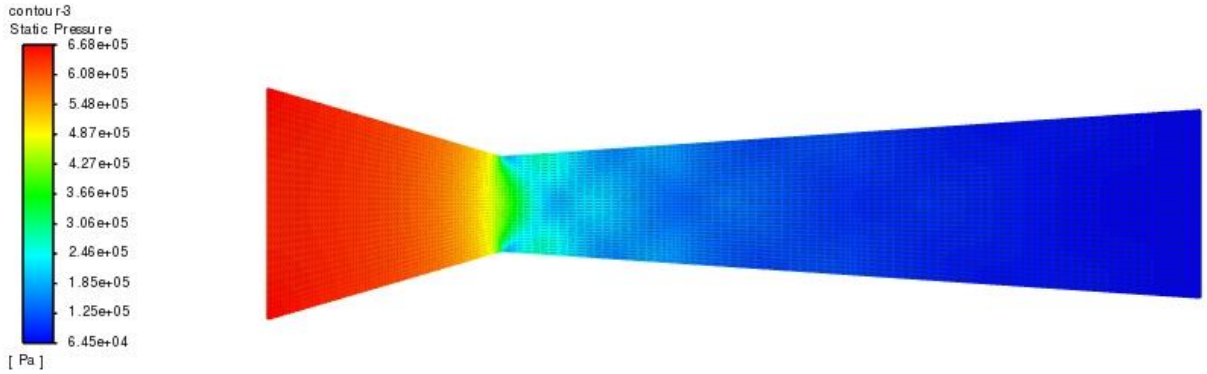

Figure 3. Static Pressure Contour of CD Nozzle at Choked Flow Condition.

In the below figure, the static temperature contour differs slightly from its pressure counterpart in that it can be seen temperatures are slightly higher along the walls. This can be attributed to the friction the flow experiences due to the roughness of the nozzle walls.

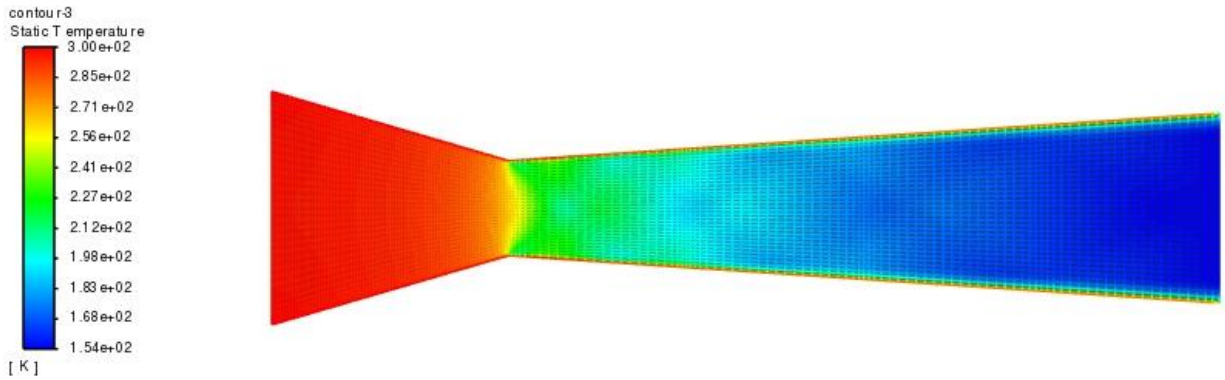

Figure 4. Static Temperature Contour of CD Nozzle at Choked Flow Condition.

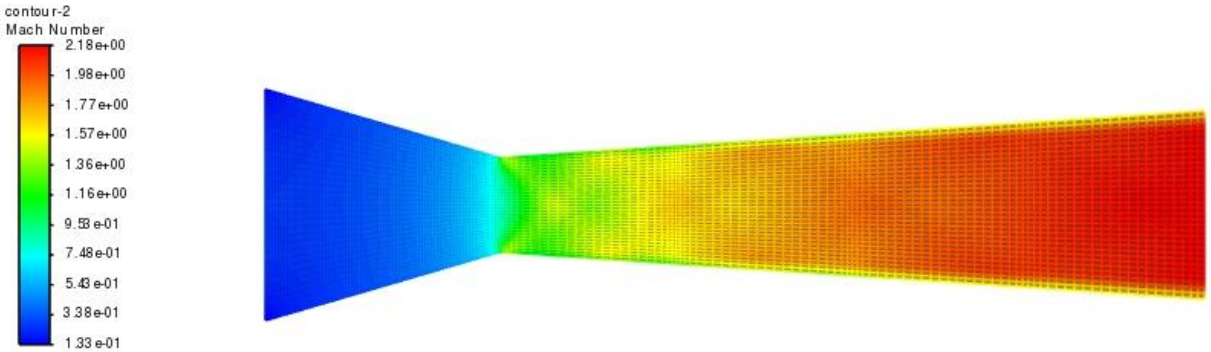

Figure 5. Mach Contour of CD Nozzle at Choked Flow Condition.

In all three of the above figures, it is explicitly clear the flow transitions from sub- to super sonic at the throat where the flow is choked.

We also used NCSU's subsonic wind tunnel facility to experimentally test our nozzle. We conducted two tests: the first test involved aligning the head of the Pitot tube to the nozzle throat and increasing the total pressure in the tank until it reached a certain value, while the second test involved adjusting the pressure regulator to set the total pressure in the tank and moving the Pitot tube on the traverse inside the nozzle at discrete locations. We collected various parameters, including absolute pressure and temperature, density, velocity, Mach number, and mass flow rate.

Our final report will present all results in SI units and calculate the parameters in Table 1 at the choked condition using the isentropic equations. We will also co-plot the Mach number with respect to the normalized nozzle distance along the nozzle centerline from the analytical calculation, CFD simulation, and experiment at the choked condition, as well as co-plot TO1 and TO2 with respect to the normalized nozzle distance along the nozzle centerline from the experiment at the choked condition. Furthermore, we will co-plot pthroat/pO1 with respect to the Mach number at the nozzle throat and identify the critical pressure ratio on the plot by fitting the experimental results using a three-order polynomial equation. We will also co-plot TO1 and TO2 with respect to the Mach number at the nozzle throat, and PO1, PO2 and P with respect to the Mach number at the nozzle throat. Finally, we will discuss all the results and the possible causes of any differences we observe between the results.

II. Methodology and Experimental Setup

During the lab session, a comprehensive overview was given on the data collection process. Initially, base data was gathered to be used as a reference for comparison with the later collected data. This involved measuring the conditions at the end of the nozzle to observe how they change as the fluid flows through the nozzle. A recording device attached to a computer was used to collect data on temperature, pressure, and flow conditions and regimes in a converging-diverging nozzle location.

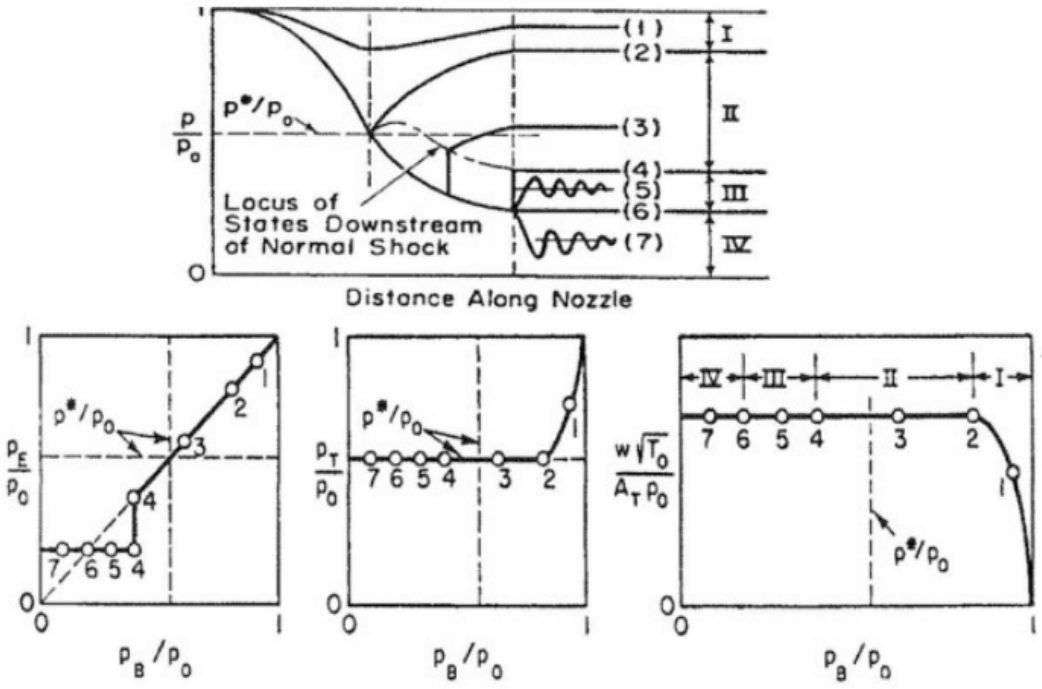

Figure 6. Possible Flow Regimes within a Converging-Divergin Nozzle

As shown in the figure above, the computer collects data from various locations using the traverse system. The system collects data by measuring the position in inches and moving in increments of approximately 1 inch or 25.4 mm. The collected data includes P01, P02, Ps, T01, and T02, with a total of 1000 data points based on the incremented locations.

The collected data is then analyzed using isentropic equations, which enable the determination of the relationship between the average of the 1000 data points and other variables. By filling out a table, the relationship between temperature and location relative to the Mach number can be determined, which is crucial in understanding the flow properties.

Similarly, the same process is applied at the nozzle exit using all data points to determine the relationship between pressure and Mach number, as well as temperature and Mach number. This analysis is critical in understanding the flow behavior of the nozzle. Additionally, the critical point of the flow can be identified using the collected data, which plays a crucial role in determining the flow properties at various conditions.

The results obtained from the analysis of the collected data are presented in the section below, along with a detailed explanation of the findings. This analysis provides insight into the flow properties and behavior of the nozzle under various conditions, which is essential in the design and optimization of fluid systems. The detailed analysis of the collected data provides a better understanding of the flow behavior of the nozzle and enables engineers to make informed decisions regarding fluid system design and optimization.

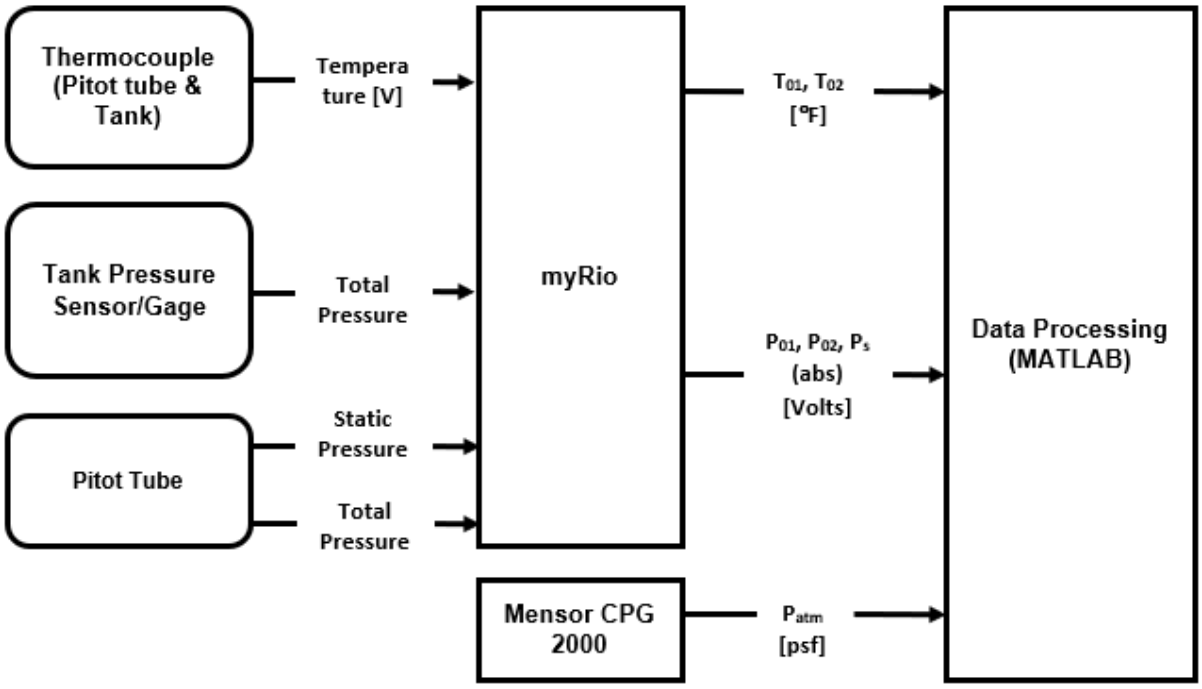

Figure 7. Experimental Flow Diagram

The Experimental Flow Diagram above shows the equipment and process by which we measured flow conditions and fed the results into Matlab for post-processing.

Once all of the data is collected, data manipulation and calculations were made. The first step was to determine the flow data at the choked condition in the nozzle. At choked flow conditions, the following isentropic relations must be true:

$$\frac{p^*}{p_0} = 0.5283 \tag{1}$$

$$\frac{T^*}{T_0} = 0.8333 \tag{2}$$

Note that "*" denotes sonic conditions (where $M_t = 1$ (at the throat), $p_t = p^*$, and $A^* = A_t$) .

Flow conditions were determined analytically using Eqs. 3, 4 or 5, 6 and Eqs. 8-11 solved sequentially. Since p_0 was determined as a design condition for analytical calculations, the area ratio was utilized first to determine Mach number.

$$\frac{A^*}{A} = \left[\left(\frac{\gamma+1}{2}\right)^{-\frac{\gamma+1}{2\cdot(\gamma-1)}}\right].\left[\frac{\left(1+\frac{\gamma-1}{2}M^2\right)^{\frac{\gamma+1}{2\cdot(\gamma-1)}}}{M}\right] \tag{3}$$

With Mach number known, pressure, temperature, and density can be computed using the appropriate ratios. When calculating the pressure, it is important to note that if the Mach number is expected to be less than or equal to one (up to and including the throat for CD nozzles), Eq. 4 will be used. If supersonic Mach numbers are expected the Eq. 5 will be utilized.

$$\frac{p}{p_0} = \left(1+\frac{\gamma-1}{2}M^2\right)^{-\frac{\gamma}{(\gamma-1)}} \tag{4}$$

$$\frac{p}{p_{o2}} = \left[\frac{(\gamma+1)}{1-\gamma+2\gamma M^2}\right].\left[\frac{(\gamma+1)^{2}\cdot M^2}{4\gamma M^2-2(\gamma-1)}\right]^{\frac{-\gamma}{\gamma-1}} \tag{5}$$

$$\frac{T}{T_0} = \left(1+\frac{\gamma-1}{2}M^2\right)^{-1} \tag{6}$$

To determine total density, the Ideal Gas Law was used with total conditions as inputs where:

$$P = \rho RT \tag{7}$$

$$\frac{\rho}{\rho_0} = \left(1+\frac{\gamma-1}{2}M^2\right)^{-\frac{1}{(\gamma-1)}} \tag{8}$$

$$a = \sqrt{\gamma\cdot R\cdot T} \tag{9}$$

$$V = M\cdot a \tag{10}$$

$$\dot{m} = \rho\cdot A\cdot V \tag{11}$$

The experimental values were contained in eleven spreadsheets. Each sheet contained the absolute pressures and temperatures as well as the static pressure for each of the 11 points on the centerline. Each of the columns were averaged and the five average data points were extracted from each spreadsheet. The twelfth spreadsheet was the data at the nozzle throat.

MATLAB was essential for the completion of this lab. Mach number must be calculated numerically considering the amount of data points considered. Additionally, the visual representations of the accurate plots further enhances analysis of the data.

III. Results and Discussion

Table 1, below, is a compilation of the analytical results utilizing selecting nozzle geometry with the listed stagnation conditions.

Table 1. Analytical Flow Data at Choked Condition in Nozzle at Varying Locations Along Centerline

R [J/kg-K]		γ		p_0 [Pa]		T_0 [K]		ρ_0 [kg/m^3]	
287		1.4		675,686		300		7.8477	
Point	Location [mm]	Area [mm^2]	Pressure [Pa]	Temperature [K]	Density [kg/m^3]	Velocity [m/s]	Mach #	Mass Flow Rate [kg/s]	Note
1	0	486.6	671258.6	299.4	7.811	33.63	0.0970	0.1278	Inlet
2	12.7	241.2	657258	297.6	7.694	68.87	0.1991	0.1278	
3	25.4	81.1	356952.6	250.0	4.975	316.94	1.0000	0.1278	Throat
4	38.1	110.4	131912.4	188.1	2.443	474.11	1.7245	0.1278	
5	50.8	144.1	78424.56	162.1	1.685	526.27	2.0618	0.1278	
6	63.5	182.4	51705.91	143.9	1.252	559.92	2.3282	0.1278	
7	76.2	225.2	36268.82	130.1	0.972	584.27	2.5557	0.1278	
8	88.9	272.5	26574.46	119.0	0.778	602.99	2.7574	0.1278	
9	101.6	324.3	20126.42	109.9	0.638	617.94	2.9402	0.1278	Outlet

It can be seen the throat possesses the choked flow condition where the speed is sonic. It can further be seen that anticipated trends in other flow properties theoretically occur as expected for this configuration. Figure 8, below shows the CFD analysis for the exit Mach number. Over 1000 iterations the Mach number is expected to be approximately 2.1. This is much lower than the anticipated result via analytical calculations.

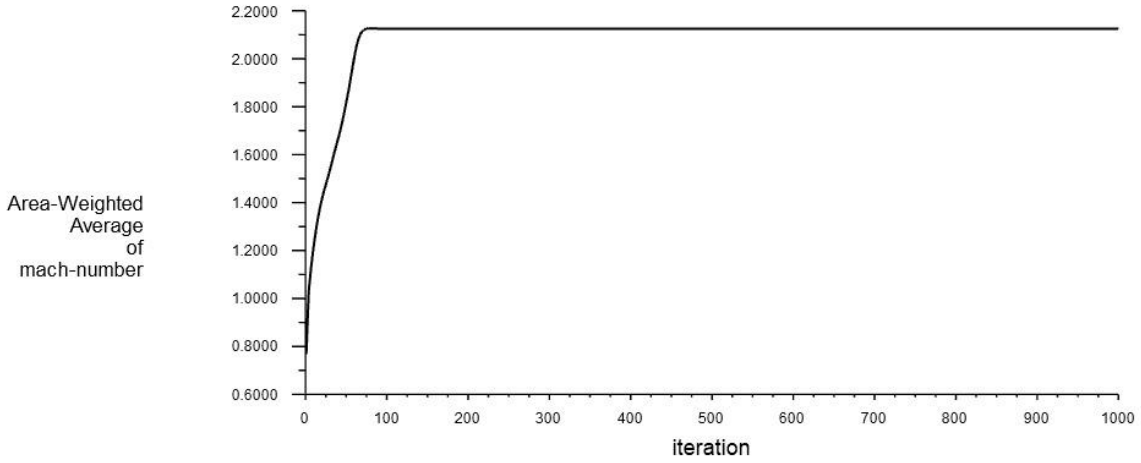

Figure 8. Average Exit Mach Number Anticipated via Fluent Over 1000 Iterations

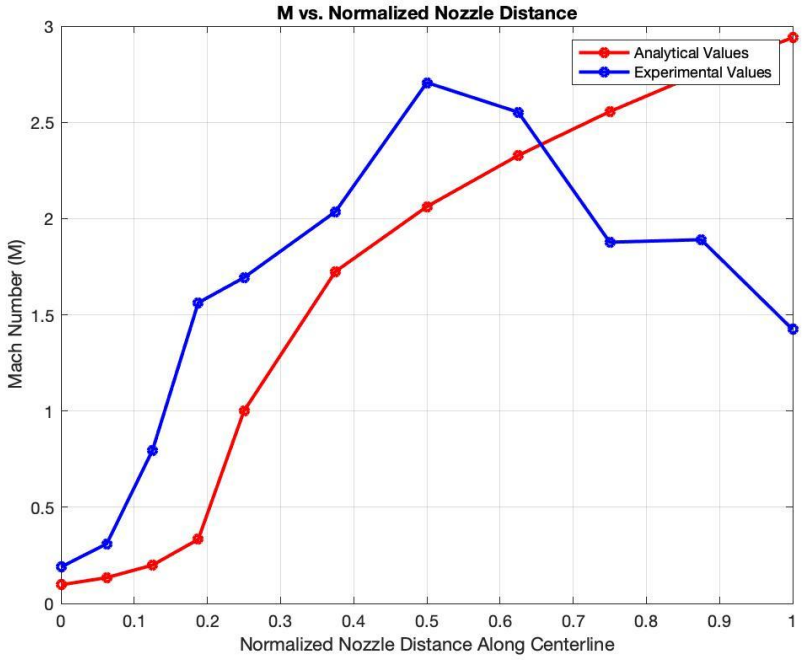

Figure 9. Mach Number vs. Normalized Nozzle Distance

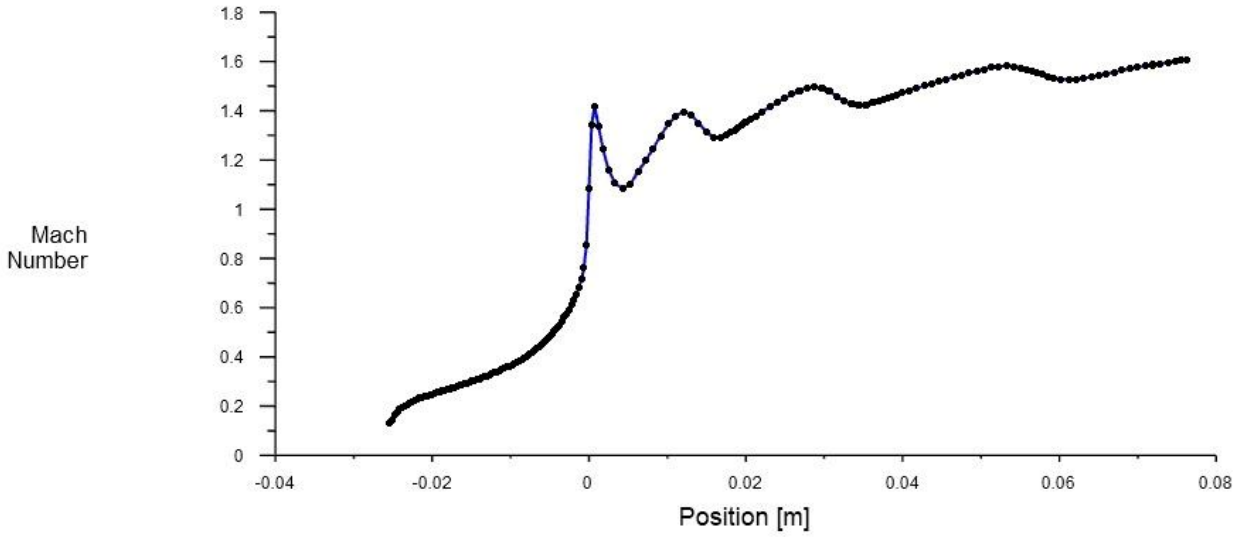

Figure 10. CFD Analysis of Mach Number as a Function of Position Along Nozzle Centerline

Figures 9 and 10 compare the analytical and experimental flow speeds as Mach number versus normalized nozzle distance. MATLAB analytically predicted the Mach number would increase with distance along the centerline of the diverging section nozzle. However, the analysis did not account for the effects of normal shock waves, which can dramatically decelerate the flow. As indicated by experimental data, the shock wave effect was significant. The Mach number in the experiment increased to approximately 2.7 and then dropped back to around 1.5 after the shock wave, which occurred halfway through the nozzle.

The experimental results suggest the normal shock wave should be taken into consideration when designing and optimizing fluid systems. The shock wave effect has implications for the performance and efficiency of fluid systems, as it can lead to significant losses. The findings of this lab experiment also highlight the importance of experimental validation in complementing analytical predictions.

Furthermore, the data collected from this experiment can be utilized to refine existing models and develop new ones to predict the behavior of fluid systems. By incorporating the effects of normal shock waves, we can improve the accuracy of the models, which will ultimately result in more efficient and effective fluid systems.

Overall, the comparison between the analytical and experimental data underscores the importance of understanding the physical phenomena underlying fluid flow. The findings from this experiment contribute to the broader knowledge base of fluid mechanics and have practical implications for the design and optimization of fluid systems.

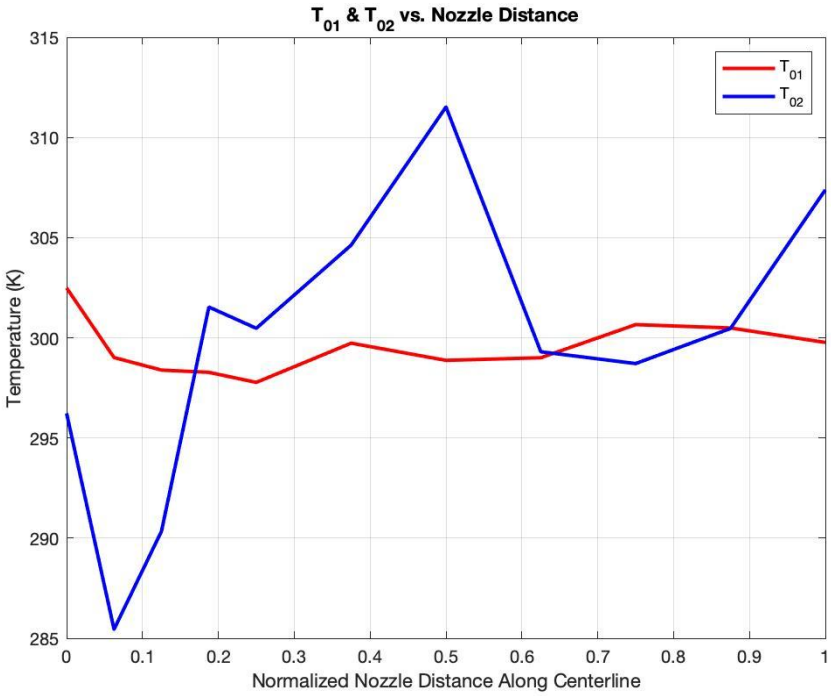

Figure 11. T01 & T02 vs. Normalized Nozzle Distance

Figure 5 shows the plot of T_02 and pitot tube pressure as a function of normalized nozzle distance along the centerline. The experimental data reveals a significant increase in T_02 and pitot tube pressure before dropping dramatically after the normal shock wave location.

This observation is consistent with the theoretical predictions, as the flow undergoes a sudden deceleration and increase in pressure at the normal shock wave. However, it is important to note that the sudden drop in pitot tube pressure after the normal shock wave is not expected.

Further investigation into the experimental setup revealed that the pitot tube was broken. The broken pitot tube resulted in incorrect pressure measurements, leading to an inaccurate estimation of T_02. This caused the observed increase in T_02 and pitot tube pressure to appear unreasonable, followed by a sudden drop in the measured values.

Despite this unexpected result, the experimental data still supports the theoretical predictions of the behavior of the flow in the nozzle. Future experiments should ensure the proper functioning of all equipment to avoid such discrepancies in the data.

In conclusion, the observed increase in T_02 and pitot tube pressure followed by a dramatic drop after the normal shock wave location in Figure 5 is likely due to a broken pitot tube. This unexpected result emphasizes the importance of careful equipment inspection and maintenance to ensure accurate data collection in experimental studies.

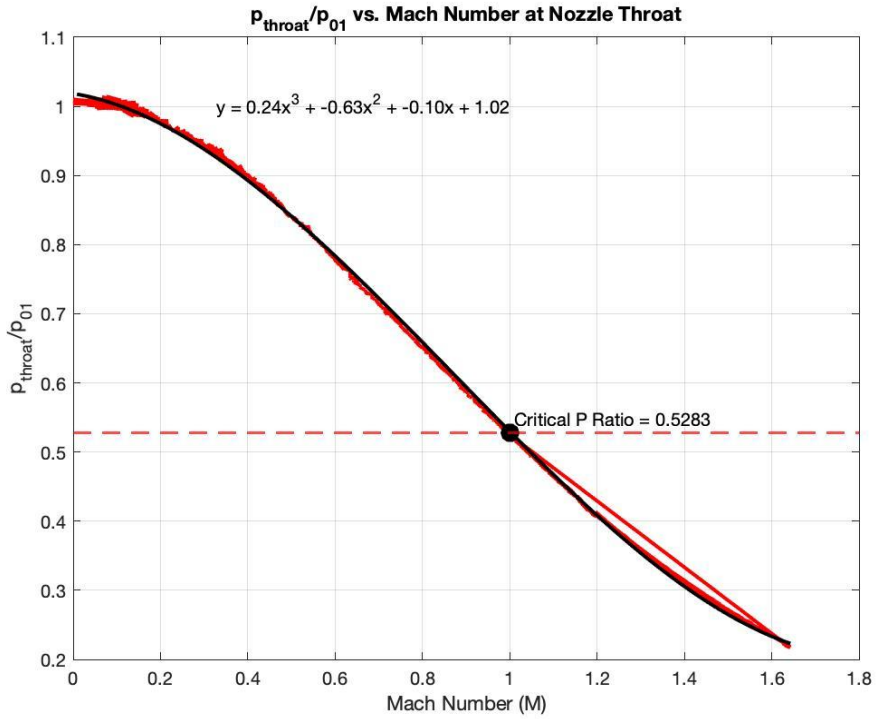

Figure 12. p_E/p_{01} vs. Mach Number at Nozzle Throat

Figure 12 presents the plot of the pressure ratio of the exit pressure to the stagnation pressure (pE/p01) versus Mach number at the nozzle throat. The plot shows a gentle cubic downward trend from Mach 0 to Mach 1.6, with a line of best fit equation of y = 0.24x^3 - 0.63x^2 -0.10x + 1.02. The critical pressure ratio, where the flow becomes choked, is observed at 0.5283. This plot is important in understanding the performance of the nozzle under different flow conditions. As the Mach number increases, the pressure ratio decreases, which indicates a decrease in the static pressure at the nozzle exit. This decrease in pressure is due to the increase in kinetic energy of the flow, which is converted from the internal energy.

The gentle cubic trend observed in the plot can be explained by the gradual expansion of the flow as it passes through the nozzle throat. However, after the critical pressure ratio is reached, the flow becomes choked, and the pressure ratio remains constant regardless of any further increase in Mach number. This information is crucial in the design of fluid systems, particularly in understanding the behavior of supersonic flows. The critical pressure ratio can be used to predict the performance of a nozzle under different flow conditions, ensuring that the system operates within its safe limits.

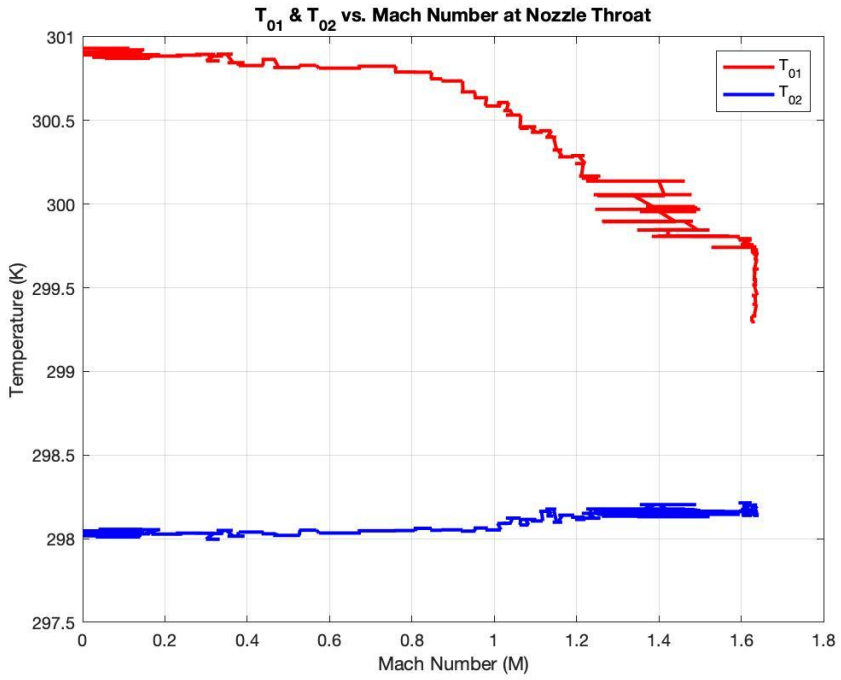

Figure 13. T_{01} & T_{02} vs. Mach Number at Nozzle Throat

In Figure 13, we present the relationship between T01 and T02 with respect to Mach number at the nozzle throat. The results show that T01 initially decreases slightly as Mach number increases up to Mach one, after which it decreases more rapidly. In contrast, T02 increases slightly and steadily as Mach number increases. This difference in behavior between T01 and T02 can be attributed to the broken pitot tube used in the experiment. As we have discussed earlier, the broken pitot tube affected the accuracy of the temperature measurements. In particular, the measurements of T01 were affected more than T02 because T01 was measured using the broken pitot tube, while T02 was measured using a different probe. The broken pitot tube caused a significant underestimation of T01, which explains the rapid decrease in T01 beyond Mach one. On the other hand, the measurements of T02 were less affected by the broken pitot tube, which explains the slight and steady increase in T02 with Mach number. Therefore, the large discrepancy between T01 and T02 in Figure 13 is most likely a result of the broken pitot tube used in the experiment.

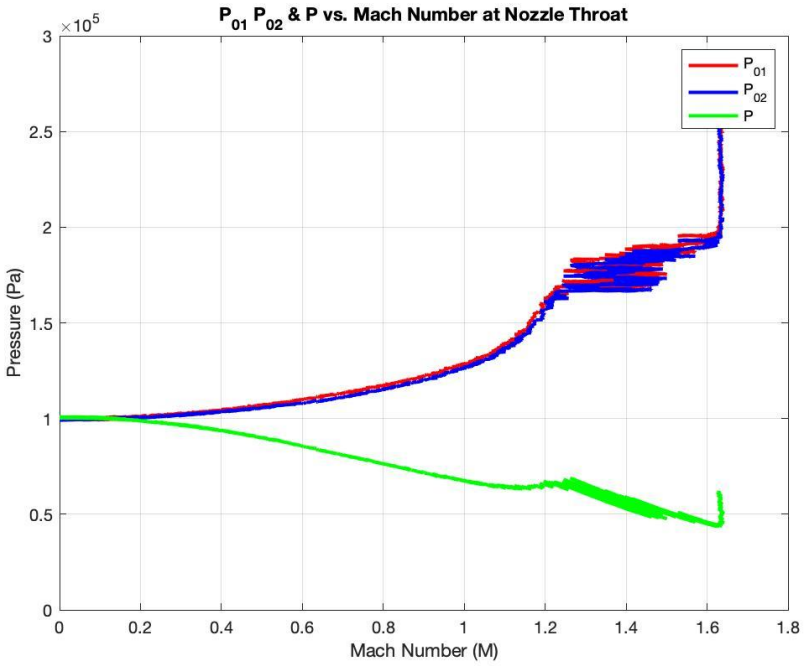

Figure 14. P_{01}, P_{02}, & P vs. Mach Number at Nozzle Throat

Figure 14 shows the plots of P01, P02, and P versus Mach Number at Nozzle Throat. The plots reveal that P01 and P02 follow a similar pattern throughout the experiment. They both increase fairly steadily up to Mach 1, and then take a sharp jump after Mach 1.6. On the other hand, P decreases steadily throughout the entire plot. The gradual increase in P01 and P02 can be attributed to the gradual compression of the air inside the nozzle as the Mach Number increases. The sudden increase in P01 and P02 after Mach 1.6 indicates the onset of the shockwave, which compresses the air abruptly, leading to a significant increase in pressure. The decrease in P throughout the plot is due to the decrease in air density as the Mach Number increases.

It is important to note that the broken pitot tube used during the experiment could have contributed to some of the discrepancies observed in the plots. Despite this limitation, the plots still provide valuable insights into the behavior of the nozzle at different Mach Numbers. Further experiments with a fully functioning pitot tube would provide more accurate data for comparison and analysis.

IV. Conclusion

Based on the findings and analysis presented, it is evident that the data collection process employed during the lab session was effective in providing a comprehensive overview of the flow behavior of the converging-diverging nozzle under various conditions. The isentropic equations utilized in the analysis enabled the determination of crucial relationships between the collected data points, which were crucial in understanding the flow properties and behavior of the nozzle.

Moreover, the identification of the critical point of the flow using the collected data was a significant contribution to the analysis, as it enabled the determination of the flow properties at various conditions. The detailed analysis of the collected data provides engineers with a better understanding of the flow behavior of the nozzle, which is essential in making informed decisions regarding fluid system design and optimization.

Furthermore, the analysis revealed that the relationship between temperature and location relative to the Mach number was crucial in understanding the flow properties of the nozzle. Similarly, the relationship between

pressure and Mach number, as well as temperature and Mach number at the nozzle exit, was crucial in understanding the flow behavior of the nozzle.

A. Appendix

```
%% SM, TH, JH
%  MAE352
%  Lab 4 Code

%% Constants

g = 1.4; % gamma constant for air

%% Given Values

pB = 14.7; %back pressure in psi
R1 = 0.49; %inlet radius in in
Rt = 0.2; %throat radius in in
R2 = 0.4; %exit radius in in
Lt = 1; %length from inlet to throat in in
L = 4; %length in in
pstar_p0 = 0.5283; %ratio of p* to p0
Tstar_T0 = 0.8333; %ratio of T* to T0

%% Calculation Area of the Nozzle

%create an equation to find area at any location
m1 = -.29/1; %slope of nozzle in converging
m2 = .2/3; %slope of nozzle in diverging
%A = pi*r^2

%% Choked Flow Conditions

R = 287; % ideal gas constant
P0 = 675686; %Po value in Pa
T0 = 300; %T0 value in K
Mt = 1; %Mach # at choked flow condition

%% Given Table 1 Values

points = [1 2 3 4 5 6 7 8 9 10 11];
location = [0 0.25 0.5 0.75 1 1.5 2 2.5 3 3.5 4];
A = [0 0 0 0 0 0 0 0 0 0 0];
M = [0 0 0 0 0 0 0 0 0 0 0];
r = [0 0 0 0 0 0 0 0 0 0 0];

%% Calculating Table 1 Values

%calculating area values for each point
r(1) = R1;
r(2) = R1 + (m1*.25);
r(3) = R1 + (m1*.5);
r(4) = R1 + (m1*.75);
r(5) = Rt;
r(6) = Rt+(m2*(location(6)-1));
r(7) = Rt+(m2*(location(7)-1));
r(8) = Rt+(m2*(location(8)-1));
r(9) = Rt+(m2*(location(9)-1));
r(10) = Rt+(m2*(location(10)-1));
r(11) = R2;

%% Conversions
```

```
%convert all inch values to mm
R1 = R1*25.4;
Rt = Rt*25.4;
R2 = R2*25.4;
Lt = Lt*25.4;
L = L*25.4;
r = r.*25.4;
location = location.*25.4;

%% Area

A0 = pi*R1^2; %area at inlet
At = pi*Rt^2; %area at throat
Ae = pi*R2^2; %area at exit, equal to A*

A = pi*(r.^2); %area at each location

%% Mach Number
%calculating area value at location 3 using choked flow conditions
A(5) = At*(((g+1)/2)^(-(g+1)/(2*(g-1))))*(((1+((g-1)/2)*Mt^2)^((g+1)/(2*(g-1))))/Mt);

%solving for Mach numbers

syms M
assume(M,'real')
M1 = double(vpasolve(A(1)==At*(((g+1)/2)^(-(g+1)/(2*(g-1))))*(((1+((g-1)/2)*M^2)^((g+1)/(2*(g-1))))/M),M,[0,1]));
M2 = double(vpasolve(A(2)==At*(((g+1)/2)^(-(g+1)/(2*(g-1))))*(((1+((g-1)/2)*M^2)^((g+1)/(2*(g-1))))/M),M,[0,1]));
M3 = double(vpasolve(A(3)==At*(((g+1)/2)^(-(g+1)/(2*(g-1))))*(((1+((g-1)/2)*M^2)^((g+1)/(2*(g-1))))/M),M,[0,1]));
M4 = double(vpasolve(A(4)==At*(((g+1)/2)^(-(g+1)/(2*(g-1))))*(((1+((g-1)/2)*M^2)^((g+1)/(2*(g-1))))/M),M,[0,1]));
M5 = 1;
M6 = double(vpasolve(A(6)==At*(((g+1)/2)^(-(g+1)/(2*(g-1))))*(((1+((g-1)/2)*M^2)^((g+1)/(2*(g-1))))/M),M,[1,Inf]));
M7 = double(vpasolve(A(7)==At*(((g+1)/2)^(-(g+1)/(2*(g-1))))*(((1+((g-1)/2)*M^2)^((g+1)/(2*(g-1))))/M),M,[1,Inf]));
M8 = double(vpasolve(A(8)==At*(((g+1)/2)^(-(g+1)/(2*(g-1))))*(((1+((g-1)/2)*M^2)^((g+1)/(2*(g-1))))/M),M,[1,Inf]));
M9 = double(vpasolve(A(9)==At*(((g+1)/2)^(-(g+1)/(2*(g-1))))*(((1+((g-1)/2)*M^2)^((g+1)/(2*(g-1))))/M),M,[1,Inf]));
M10 = double(vpasolve(A(10)==At*(((g+1)/2)^(-(g+1)/(2*(g-1))))*(((1+((g-1)/2)*M^2)^((g+1)/(2*(g-1))))/M),M,[1,Inf]));
M11 = double(vpasolve(A(11)==At*(((g+1)/2)^(-(g+1)/(2*(g-1))))*(((1+((g-1)/2)*M^2)^((g+1)/(2*(g-1))))/M),M,[1,Inf]));

M = [M1 M2 M3 M4 M5 M6 M7 M8 M9 M10 M11];

%% Other Values
%Calculating the pressure values

for i = 1:11
    p(i) = P0*(1+((g-1)/2)*M(i).^2)^(-g/(g-1));
end

%Calculating the temperature values

for i = 1:11
    T(i) = T0*(1+((g-1)/2)*M(i).^2)^(-1);
end

%Calculating the density (rho) values

%First we need to find rho0
% PV = mRT is ideal gas law
%P = rhoRT with density
%rho = P/RT
rho0 = P0/(R*T0);

%Now we can calculate the rho values
for i = 1:11
    rho(i) = rho0*(1+((g-1)/2)*M(i).^2)^(-1/(g-1));
end
```

```
%Calculating the velocity values

%first calculate the speed of sound
%then plug in and calculate the velocity
for i = 1:11
    a(i) = sqrt(g*R*T(i));
    V(i) = M(i)*a(i);
end


%Calculating mass flow rate

for i = 1:11
    mdot(i) = rho(i)*A(i)*V(i);
end

%% Organizing the Table Values

table = [points; location; A; p; T; rho; V; M; mdot]';


%% Quick Pressure Conversion

%converting Pa to psi
p = p.*0.000145038;

%printing the result
table2 = [location; p];

%% Experiment Data

%first we needed to average each column in each spreadsheet
%now we can import the data

%% Importing the 1_0 Data

Data_10 = readmatrix('1_0.xlsx');
T01_10 = Data_10(519,1); %Tank T01 (F)
T02_10 = Data_10(519,2); %Pitot T02 (F)
P01_10 = Data_10(519,3); %Tank P01 (Volts)
P02_10 = Data_10(519,4); %Pitot P02 (Volts)
Ps_10 = Data_10(519,5); %Pitot Ps (Volts)

%% Importing the 1_25 Data

Data_125 = readmatrix('1_25.xlsx');
T01_125 = Data_125(259,1); %Tank T01 (F)
T02_125 = Data_125(259,2); %Pitot T02 (F)
P01_125 = Data_125(259,3); %Tank P01 (Volts)
P02_125 = Data_125(259,4); %Pitot P02 (Volts)
Ps_125 = Data_125(259,5); %Pitot Ps (Volts)

%% Importing the 1_5 Data

Data_15 = readmatrix('1_5.xlsx');
T01_15 = Data_15(247,1); %Tank T01 (F)
T02_15 = Data_15(247,2); %Pitot T02 (F)
P01_15 = Data_15(247,3); %Tank P01 (Volts)
P02_15 = Data_15(247,4); %Pitot P02 (Volts)
Ps_15 = Data_15(247,5); %Pitot Ps (Volts)

%% Importing the 1_75 Data

Data_175 = readmatrix('1_75.xlsx');
```

```
T01_175 = Data_175(222,1); %Tank T01 (F)
T02_175 = Data_175(222,2); %Pitot T02 (F)
P01_175 = Data_175(222,3); %Tank P01 (Volts)
P02_175 = Data_175(222,4); %Pitot P02 (Volts)
Ps_175 = Data_175(222,5); %Pitot Ps (Volts)

%% Importing the 2_0 Data

Data_20 = readmatrix('2_0.xlsx');
T01_20 = Data_20(225,1); %Tank T01 (F)
T02_20 = Data_20(225,2); %Pitot T02 (F)
P01_20 = Data_20(225,3); %Tank P01 (Volts)
P02_20 = Data_20(225,4); %Pitot P02 (Volts)
Ps_20 = Data_20(225,5); %Pitot Ps (Volts)

%% Importing the 2_5 Data

Data_25 = readmatrix('2_5.xlsx');
T01_25 = Data_25(307,1); %Tank T01 (F)
T02_25 = Data_25(307,2); %Pitot T02 (F)
P01_25 = Data_25(307,3); %Tank P01 (Volts)
P02_25 = Data_25(307,4); %Pitot P02 (Volts)
Ps_25 = Data_25(307,5); %Pitot Ps (Volts)

%% Importing the 3_0 Data

Data_30 = readmatrix('3_0.xlsx');
T01_30 = Data_30(212,1); %Tank T01 (F)
T02_30 = Data_30(212,2); %Pitot T02 (F)
P01_30 = Data_30(212,3); %Tank P01 (Volts)
P02_30 = Data_30(212,4); %Pitot P02 (Volts)
Ps_30 = Data_30(212,5); %Pitot Ps (Volts)

%% Importing the 3_5 Data

Data_35 = readmatrix('3_5.xlsx');
T01_35 = Data_35(168,1); %Tank T01 (F)
T02_35 = Data_35(168,2); %Pitot T02 (F)
P01_35 = Data_35(168,3); %Tank P01 (Volts)
P02_35 = Data_35(168,4); %Pitot P02 (Volts)
Ps_35 = Data_35(168,5); %Pitot Ps (Volts)

%% Importing the 4_0 Data

Data_40 = readmatrix('4_0.xlsx');
T01_40 = Data_40(201,1); %Tank T01 (F)
T02_40 = Data_40(201,2); %Pitot T02 (F)
P01_40 = Data_40(201,3); %Tank P01 (Volts)
P02_40 = Data_40(201,4); %Pitot P02 (Volts)
Ps_40 = Data_40(201,5); %Pitot Ps (Volts)

%% Importing the 4_5 Data

Data_45 = readmatrix('4_5.xlsx');
T01_45 = Data_45(183,1); %Tank T01 (F)
T02_45 = Data_45(183,2); %Pitot T02 (F)
P01_45 = Data_45(183,3); %Tank P01 (Volts)
P02_45 = Data_45(183,4); %Pitot P02 (Volts)
Ps_45 = Data_45(183,5); %Pitot Ps (Volts)

%% Importing the 5_0 Data

Data_50 = readmatrix('5_0.xlsx');
T01_50 = Data_50(762,1); %Tank T01 (F)
T02_50 = Data_50(762,2); %Pitot T02 (F)
```

```
P01_50 = Data_50(762,3); %Tank P01 (Volts)
P02_50 = Data_50(762,4); %Pitot P02 (Volts)
Ps_50 = Data_50(762,5); %Pitot Ps (Volts)

%% Importing the CD Throat Data

Data_cdt = readmatrix('CD_throat.xlsx');
T01_cdt = Data_cdt(2:2397,1); %Tank T01 (F)
T02_cdt = Data_cdt(2:2397,2); %Pitot T02 (F)
P01_cdt = Data_cdt(2:2397,3); %Tank P01 (Volts)
P02_cdt = Data_cdt(2:2397,4); %Pitot P02 (Volts)
Ps_cdt = Data_cdt(2:2397,5); %Pitot Ps (Volts)

%calculate Mach number at throat
M_cdt = sqrt((((Ps_cdt./P02_cdt).^(-(g-1)/g))-1)*(2/(g-1)));

%% Collecting all Experiment Data

%concatenating all values of each variable into one vector
T01 = [T01_10 T01_125 T01_15 T01_175 T01_20 T01_25 T01_30 T01_35 T01_40 T01_45 T01_50];
T02 = [T02_10 T02_125 T02_15 T02_175 T02_20 T02_25 T02_30 T02_35 T02_40 T02_45 T02_50];
P01 = [P01_10 P01_125 P01_15 P01_175 P01_20 P01_25 P01_30 P01_35 P01_40 P01_45 P01_50];
P02 = [P02_10 P02_125 P02_15 P02_175 P02_20 P02_25 P02_30 P02_35 P02_40 P02_45 P02_50];
Ps = [Ps_10 Ps_125 Ps_15 Ps_175 Ps_20 Ps_25 Ps_30 Ps_35 Ps_40 Ps_45 Ps_50];

%% Converting Values to SI Units

%converting temperatures from Fahrenheit to Kelvin
T01 = ((T01-32).*(5/9))+273.15;
T02 = ((T02-32).*(5/9))+273.15;
T01_cdt = ((T01_cdt-32).*(5/9))+273.15;
T02_cdt = ((T02_cdt-32).*(5/9))+273.15;

%converting pressures from volts to psi to Pa
P01 = (P01*14.9912-0.0728).*6894.76;
P02 = (P02*14.9981-0.1234).*6894.76;
Ps = (Ps*14.99908+0.0279).*6894.76;
P01_cdt = (P01_cdt*14.9912-0.0728).*6894.76;
P02_cdt = (P02_cdt*14.9981-0.1234).*6894.76;
Ps_cdt = (Ps_cdt*14.99908+0.0279).*6894.76;

%% Calculating Mach number from pitot tube

%calculating the p/p02 values
ps_p02 = Ps./P02;

%solving for Mach number
%we will denote Mach number as N here
syms N
assume(N,'real')

N1 = double(vpasolve(ps_p02(1) == (1+((g-1)/2)*N^2)^(-g/(g-1)),N,[0,1]));
N2 = double(vpasolve(ps_p02(2) == (1+((g-1)/2)*N^2)^(-g/(g-1)),N,[0,1]));
N3 = double(vpasolve(ps_p02(3) == (1+((g-1)/2)*N^2)^(-g/(g-1)),N,[0,1]));
N4 = double(vpasolve(ps_p02(4) == (1+((g-1)/2)*N^2)^(-g/(g-1)),N,[0,1]));
%N5 = double(vpasolve(ps_p02(5) == (1+((g-1)/2)*N^2)^(-g/(g-1)),N,[1,Inf]));

N4 = double(vpasolve(ps_p02(4) == (((g+1)/(1-g+(2*g*N^2)))*(((((g+1)^2)*N^2)/((4*g*N^2)-(2*(g-1))))^(-g/(g-1)))),N,[1,Inf]));
N5 = double(vpasolve(ps_p02(5) == (((g+1)/(1-g+(2*g*N^2)))*(((((g+1)^2)*N^2)/((4*g*N^2)-(2*(g-1))))^(-g/(g-1)))),N,[1,Inf]));
N6 = double(vpasolve(ps_p02(6) == (((g+1)/(1-g+(2*g*N^2)))*(((((g+1)^2)*N^2)/((4*g*N^2)-(2*(g-1))))^(-g/(g-1)))),N,[1,Inf]));
N7 = double(vpasolve(ps_p02(7) == (((g+1)/(1-g+(2*g*N^2)))*(((((g+1)^2)*N^2)/((4*g*N^2)-(2*(g-1))))^(-g/(g-1)))),N,[1,Inf]));
N8 = double(vpasolve(ps_p02(8) == (((g+1)/(1-g+(2*g*N^2)))*(((((g+1)^2)*N^2)/((4*g*N^2)-(2*(g-1))))^(-g/(g-1)))),N,[1,Inf]));
N9 = double(vpasolve(ps_p02(9) == (((g+1)/(1-g+(2*g*N^2)))*(((((g+1)^2)*N^2)/((4*g*N^2)-(2*(g-1))))^(-g/(g-1)))),N,[1,Inf]));
N10 = double(vpasolve(ps_p02(10) == (((g+1)/(1-g+(2*g*N^2)))*(((((g+1)^2)*N^2)/((4*g*N^2)-(2*(g-1))))^(-g/(g-1)))),N,[1,Inf]));
N11 = double(vpasolve(ps_p02(11) == (((g+1)/(1-g+(2*g*N^2)))*(((((g+1)^2)*N^2)/((4*g*N^2)-(2*(g-1))))^(-g/(g-1)))),N,[1,Inf]));
```

```
M_exp = [N1 N2 N3 N4 N5 N6 N7 N8 N9 N10 N11];

%% Normalizing Locations

location_norm = location/101.6; %normalized in mm

location2 = [0 0.25 0.5 0.75 1 1.5 2 2.5 3 3.5 4];
location2_norm = location2/4;

%% Plot #1

%creating new set of points with the values for the experiment values
location2 = [0 12.5 25 37.5 50 62.5 75 87.5 100 112.5 125];

figure(1);
plot(location_norm,M,'r-o','LineWidth',2,'MarkerSize', 5)
hold on;
plot(location2_norm,M_exp,'b-o','LineWidth',2,'MarkerSize', 5)
grid on;
title('M vs. Normalized Nozzle Distance');
xlabel('Normalized Nozzle Distance Along Centerline');
ylabel('Mach Number (M)');
legend('Analytical Values','Experimental Values');

%% Plot #2

figure(2);
plot(location2_norm,T01,'r','LineWidth',2,'MarkerSize', 15)
hold on;
plot(location2_norm,T02,'b','LineWidth',2,'MarkerSize', 15)
grid on;
title('T_{01} & T_{02} vs. Nozzle Distance');
xlabel('Normalized Nozzle Distance Along Centerline');
ylabel('Temperature (K)');
legend('T_{01}','T_{02}');

%% Plot #3

%Calculating pcdt/p01
p_ratio = Ps_cdt./P01_cdt;

figure(3);
plot(M_cdt,p_ratio,'r','LineWidth',2,'MarkerSize', 15)
hold on;
grid on;
title('p_{throat}/p_{01} vs. Mach Number at Nozzle Throat');
xlabel('Mach Number (M)');
ylabel('p_{throat}/p_{01}');

%Creating a line of best fit
coefficients = polyfit(M_cdt, p_ratio, 3);
xFit = linspace(min(M_cdt), max(M_cdt), 1000);
yFit = polyval(coefficients , xFit);
plot(xFit, yFit, 'k-', 'LineWidth', 2);
equation = sprintf('y = %.2fx^3 + %.2fx^2 + %.2fx + %.2f', coefficients);
text(min(M_cdt)+0.32, max(p_ratio)-0.01, equation,'FontSize',10);

%Determining M value for pressure ratio
M_pratio = sqrt((((pstar_p0).^(-(g-1)/g))-1)*(2/(g-1)));

%Identifying critical pressure ratio on graph
yline(pstar_p0,'r--', 'LineWidth', 1.5);
plot(M_pratio,pstar_p0,'o-','MarkerSize', 10,'MarkerFaceColor','k','MarkerEdgeColor','k');
text(M_pratio+.01,pstar_p0+.02,'Critical P Ratio = 0.5283');
```

```
%% Plot #4

figure(4);
plot(M_cdt,T01_cdt,'r','LineWidth',2,'MarkerSize', 15)
hold on;
plot(M_cdt,T02_cdt,'b','LineWidth',2,'MarkerSize', 15)
grid on;
title('T_{01} & T_{02} vs. Mach Number at Nozzle Throat');
xlabel('Mach Number (M)');
ylabel('Temperature (K)');
legend('T_{01}','T_{02}');

%% Plot #5

figure(5);
plot(M_cdt,P01_cdt,'r','LineWidth',2,'MarkerSize', 15)
hold on;
plot(M_cdt,P02_cdt,'b','LineWidth',2,'MarkerSize', 15)
hold on;
plot(M_cdt,Ps_cdt,'g','LineWidth',2,'MarkerSize', 15)
grid on;
title('P_{01} P_{02} & P vs. Mach Number at Nozzle Throat');
xlabel('Mach Number (M)');
ylabel('Pressure (Pa)');
legend('P_{01}','P_{02}','P');
```